INTERNATIONAL JOURNAL OF
COASTAL & OFFSHORE ENGINEERING
IJCOE No. 4 / Autumn 2016 (11-18)

Modeling and Control of Autonomous Underwater Vehicle (AUV) In Heading and Depth Attitude via PPD Controller with State Feedback

Soroush Vahid[1], Kaveh Javanmard[2]

[1]*PhD candidate, Semnan University, Soroush.vahid@semnan.ac.ir*
[2] *PhD candidate, Semnan University, kavehjavanmard@semnan.ac.ir*

ARTICLE INFO

Article History:
Received: 17 Jun. 2016
Accepted: 15 Dec. 2016

Keywords:
AUV
PPD (Proportional- Proportional – Derivative)
Pitch
Circulate
hydrodynamic

ABSTRACT

This paper focuses on design of AUV control system to control depth and pitch. Complexity and highly coupled dynamics, time-variance, and difficulty in hydrodynamic modeling and simulation, complicates the AUV modeling process and the design of proper and acceptable controller. A PD (Proportional- Derivative) controller, control the vehicle pitch and an outer P loop controller with state feedback will control the depth. The kinematic and dynamic equations will be extracted using various conditions such as the relative speed along the axis X (u), the speed along the axis Z (w), Pitch rate, forward position relative to the ground (x), depth (z), and the Pitch angle (Θ). Then we linearize the equations of motion of the AUV by choosing a suitable set of operating conditions. For effective control of the motion of AUVs, we need to design controllers based on the AUV's dynamic model. Through the control of propeller and fin's deflection, we can achieve the control system of AUVs. The simulation results indicate that developed control system is stable, competent, and efficient enough to control the AUV in tracking the two channels of heading and depth with stabilized speed.

1. Introduction

Autonomous underwater vehicle (AUV) is an unmanned submersible in different sizes. It is intended to provide scientists and researchers with simple, low-cost, medium and long-range, appropriate time response capability to collect environmental data. There are a lot of applications for AUVs, including oil industry, survey on underwater animals and plants, operations in dangerous waters, photometric survey, pipeline route survey, seabed mapping, environmental monitoring, chemical plume tracing [1], salvage and rescue requests, and so on [2]. Today the significance of AUVs can easily be understood if the Unmanned Underwater Vehicles (UUV) program for the US Navy is studied [3].

Derivation of AUV parameters is a difficult process and finally its validation demands to analyze practical test like two tank test [4] or telemetry under sea [5, 6]. However, at last, estimation of parameters has uncertainty and variation; therefore, the controller must be self-tuning and robust in counter to variation of AUV parameters and also unpredictable environmental disturbances.

Inherently, nonlinear dynamics of AUVs make it more difficult to exert commonly used linear control. The dynamic characteristics of an AUV are quite complex due to its high nonlinearity, time-varying dynamic behavior, uncertainties in hydrodynamic coefficients, and disturbances caused by sea currents and waves.

Throughout the years various models of control techniques have been proposed. This includes linear controllers [1, 2, 7, 8, 10, 23], which have performed satisfactorily; SMC controllers [11, 13], adaptive control [12, 13, 20], FLC (Fuzzy Logic Control) [14], predictive control [18– 19], static feedback control [25], and neural-network-based control [15–17] have also shown good robustness and tuning ability. Since almost all control methods have some pros and cons, a proper controller can be achieved by the combination of classical and modern intelligent method.

One of the most important disadvantages of linear controllers like LQR and LQG is that they are unable to account for the nonlinearities of the system, thus they can result in suitable performance and even instability in high maneuver treatments.

Also, neural network has some weak points that bind its improvement. It converges to a precise model with long training time and slow rate, which is not acceptable by many systems. Also, classical neural network does not qualify the main requirements such as fast response, less overshoot–undershoot.

[DOR: 20.1001.1.25382667.2016.4.0.3.7]

SMC is an earlier method that is a good solution for nonlinear system but it can cause chattering on actuators, waste energy, and make fault on fins. However, there are some methods like combination with fuzzy or changing the sign functions by saturation function to reduce chattering.

The FLC is easy to use in industrial process because of its simple control structure, easy and cost-effective design [24]. However, FLC with fixed scaling factors and fuzzy rules may not give complete performance if the controlled plant has uncertainty and high nonlinearity [24]. Traditional FLC can have errors in steady state if the system does not have an inherent integrating property. Modern controllers are more robust to dynamic variations and can offer better performance index than classical controllers; however, they may require neat to exact models. The main aim of this paper is to develop an attitude control system of an AUV based on Myring hull profile via using PPD controller with state feedback. The goals are to:

1. Understand the general dynamic and kinematic of AUV by using MATLAB 2014
2. Achieve a suitable and simple controller to control heading and depth
3. Simulate the AUV's maneuvers (Snake and Spiral) and analyze the performance and accuracy of controller.

The advantage of using a PID controller is it is simple to implement and maintain, however, it is primarily applicable for linear time-invariant systems, though many extensions to nonlinear systems have been made such as [21] and references therein.

2. Model description

2.1. Coordinate systems and kinematic and dynamic equations of motion

Generally, the motion of an AUV can be introduced by six degrees of freedom (6-DOF) differential equations of motion [4], [22]. These equations are developed using two coordinate frames shown in Fig. 1. Six velocity components [u, v, w, p, q, r] (surge, sway, heave velocity, roll, pitch rate, yaw rate) are defined in the body fixed frame, while the earth-fixed frame defines the corresponding attitudes and positions [x, y, z, ϕ, θ, and ψ]. It is listed in Table 1. The axis is right-handed. The origin of the body-fixed coordinate system is center of mass.

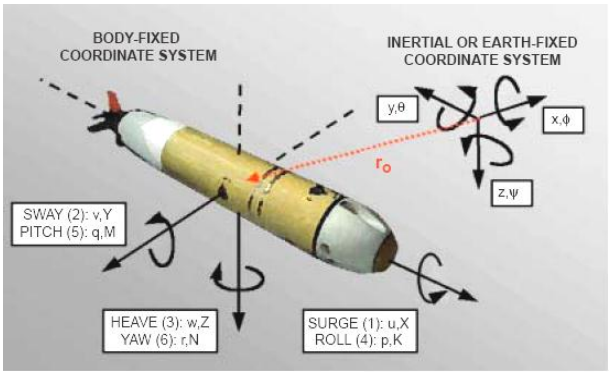

Fig. 1 Reference frame of AUV[16]

Table 1 Symbols used to describe 6-DOF

DOF	Motion	Forces and moments	velocity	Positions and Euler angles
1	surge	X	u	x
2	sway	Y	υ	y
3	Heave	Z	w	z
4	roll	K	P	ϕ
5	Pitch	M	q	θ
6	Yaw	N	r	ψ

The AUV motion is described by these vectors:

$$\eta = \begin{bmatrix} \eta_1 \\ \eta_2 \end{bmatrix} \quad \eta_1 = \begin{bmatrix} x \\ y \\ z \end{bmatrix} \text{position vector} \quad \eta_2 = \begin{bmatrix} \phi \\ \theta \\ \psi \end{bmatrix} \text{Euler angles vector} \tag{1}$$

$$\nu = \begin{bmatrix} \nu_1 \\ \nu_2 \end{bmatrix} \quad \nu_1 = \begin{bmatrix} u \\ v \\ w \end{bmatrix} \text{linear velocity vector} \quad \nu_2 = \begin{bmatrix} p \\ q \\ r \end{bmatrix} \text{angular velocity vector} \tag{2}$$

$$\tau = \begin{bmatrix} \tau_1 \\ \tau_2 \end{bmatrix} \quad \tau_1 = \begin{bmatrix} X \\ Y \\ Z \end{bmatrix} \text{forces vector} \quad \tau_2 = \begin{bmatrix} K \\ M \\ N \end{bmatrix} \text{moments vector} \tag{3}$$

It should be considered that in order to avoid singularity in circulation and transformation, Euler angles should be in this boundary:

$$\begin{aligned} &\mathbf{0} \le \psi < \mathbf{2}\pi \\ &{}^{-\pi}/_{2} < \theta < {}^{\pi}/_{2} \\ &-\pi < \phi \le \pi \end{aligned} \tag{4}$$

Transformation between these two coordinate systems is as follows:

[DOR: 20.1001.1.25382667.2016.4.0.3.7]

$$J_1(\eta_2)=C_{z,\psi}^T * C_{y,\theta}^T * C_{x,\varphi}^T = \begin{bmatrix}\cos(\psi) & -\sin(\psi) & 0\\ \sin(\psi) & \cos(\psi) & 0\\ 0 & 0 & 1\end{bmatrix}\begin{bmatrix}\cos(\theta) & 0 & \sin(\theta)\\ 0 & 1 & 0\\ -\sin(\theta) & 0 & \cos(\theta)\end{bmatrix}\begin{bmatrix}1 & 0 & 0\\ 0 & \cos(\phi) & -\sin(\phi)\\ 0 & \sin(\phi) & \cos(\phi)\end{bmatrix} \quad (5)$$

$$J_1(\eta_2)=\begin{bmatrix}\cos\theta.\cos\psi & \sin\phi.\sin\theta.\cos\psi-\cos\phi.\sin\psi & \cos\phi.\sin\theta.\cos\psi+\sin\phi.\sin\psi\\ \cos\theta.\sin\psi & \sin\phi.\sin\theta.\sin\psi+\cos\phi.\cos\psi & \cos\phi.\sin\theta.\sin\psi-\sin\phi.\cos\psi\\ -\sin\theta & \sin\phi.\cos\theta & \cos\phi.\cos\theta\end{bmatrix} \quad (6)$$

For transformation of linear velocities, by the following matrix equation time rate of the displacements described with respect to world coordinate (earth-fixed) frame rates can be obtained as follows:

$$\begin{bmatrix}\dot{x}\\ \dot{y}\\ \dot{z}\end{bmatrix}=J_1(\eta_2).\begin{bmatrix}u\\ v\\ w\end{bmatrix} \quad (7)$$

Inversely, body coordinate frame velocities can be determined from world coordinate frame velocities in a similar fashion:

$$\nu_1=J_1^{-1}(\eta_2).\dot{\eta}_1 \quad (8)$$

Angular rates described with respect to body-fixed frame are transformed into the time rate of Euler angles by following non-orthogonal transformation matrix.

$$\dot{\phi}=p+q\sin(\phi)\tan(\theta)+r\cos(\phi)\tan(\theta) \quad (9)$$

$$\dot{\theta}=q\cos(\phi)-r\sin(\phi) \quad (10)$$

$$\dot{\psi}=\frac{q\sin(\phi)+r\cos(\phi)}{\cos(\theta)} \quad (11)$$

These three equation forms are represented in matrix notation:

$$\begin{bmatrix}\dot{\phi}\\ \dot{\theta}\\ \dot{\psi}\end{bmatrix}=J_2(\eta_2).\begin{bmatrix}p\\ q\\ r\end{bmatrix} \quad (12)$$

$$J_2(\eta_2)=\begin{bmatrix}1 & \sin(\phi)\tan(\theta) & \cos(\phi)\tan(\theta)\\ 0 & \cos(\phi) & -\sin(\phi)\\ 0 & \sin(\phi)\sec(\theta) & \cos(\phi)\sec(\theta)\end{bmatrix} \quad (13)$$

2.2 the final equations for the AUV's motion simulation

Six kinematic equations of motion are as follows:

$$\begin{aligned}\dot{\phi}&=p+q\sin\phi\tan\theta+r\cos\phi\tan\theta\\ \dot{\theta}&=q\cos\phi-r\sin\phi\\ \dot{\psi}&=(q\sin\phi+r\cos\phi)/\cos\theta\end{aligned} \quad (14)$$

$$\begin{aligned}\dot{x}&=u(\cos\theta\cos\psi)+\\ &\quad v(\sin\varphi\sin\theta\cos\psi-\cos\varphi\sin\psi)+\\ &\quad w(\cos\varphi\sin\theta\cos\psi+\sin\varphi\sin\psi)\\ \dot{y}&=u(\cos\theta\sin\psi)+\\ &\quad v(\sin\varphi\sin\theta\sin\psi+\cos\varphi\cos\psi)+\\ &\quad w(\cos\varphi\sin\theta\sin\psi-\sin\varphi\cos\psi)\\ \dot{h}&=-\dot{z}=u(\sin\theta)+\\ &\quad v(-\sin\varphi\cos\theta)+\\ &\quad w(-\cos\varphi\cos\theta)\end{aligned} \quad (15)$$

3. Controller Design:

Based on the linear model containing 3 states, we will design a proportional - derivative (PD) inner loop for controlling the pitch angle θ, and a proportional (P) outer loop for controlling the depth z.

3.1. Vessel Transfer Function

The first step to design control system for a vehicle is obtain its transfer function. At first, we want to achieve the inner loop transfer function that relating input stern angle (f_s) to the output vehicle pitch angle (Θ). According to kinematic and dynamic equations expressed, the inner Pitch loop transfer function is as follows:

$$G_\theta(s)=\frac{\theta(s)}{f_s(s)}=\frac{\frac{M_{f_s}}{I_y-M_q}}{s^2-\frac{M_q}{I_y-M_q}s-\frac{M_\theta}{I_y-M_q}} \quad (16)$$

Now we calculate outer depth loop transfer function that relating the input Pitch angle (θ_d) to vehicle depth (z). Under real conditions, the inner Pitch loop response is much faster than the outer depth loop so we can make equal with Θ. According to kinematic and dynamic equations expressed, the depth transfer function is as follows:

$$G_z(s)=\frac{Z(s)}{\theta(s)}=\frac{-\mu_1}{s} \quad (17)$$

3.2. Control Law

As denoted before, we want design a proportional-derivative (PD) inner loop for controlling the pitch angle Θ and a proportional (P) for controlling the depth z. According to the control law presented above, the inner loop control law is as follow:

$$\frac{f_s(s)}{e_\theta(s)}=-K_p(T_d s+1) \quad (18)$$

Where

$$e_\theta(error\ in\ pitch)=\theta_{des}(desired\ pitch)-\theta(actual\ pitch) \quad (19)$$

Kp is proportional gain and Td is derivative time constant. Because of difference between the vehicle stern angle and pitch angle the minus sign is applied. Positive stern angle create negative torque around Y

[DOR: 20.1001.1.25382667.2016.4.0.3.7]

axis that force the vehicle diving down (negative pitch rate).
The control law for outer loop denoted as follow:

$$\Delta = \frac{\theta(s)}{e_z(s)} \quad (20)$$

Where

$$e_z = z_d - z \quad (21)$$

In view of the above control equations and considering the dynamic and kinematic characteristics of our AUV model, we designed the vehicle P-PD controller system blocks that shown as below :

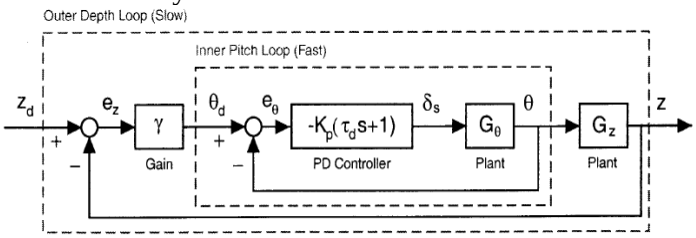

Fig.2 The vehicle controller system block

3.3. Controller design procedure:

Before choosing gain of the controller for a specified vessel we review the controller design.
We design our own controller to have a specified second order answer in natural frequency ω_n and damping coefficient ζ. For second order answer we have:

$$G(s) = \frac{K}{S^2+2\zeta\omega s+\omega^2} \quad (22)$$

3.4. Overshoot, ts, t_p

For choosing a suitable answer in a specified system, we must consider the %OS, setting time (t_s) and peak time (t_p).
Damping coefficient is a function of the percentage overshoot that calculated as follows:

$$\zeta = \frac{-\ln(\frac{\%OS}{100})}{\left[\pi^2+ln^2(\frac{\%OS}{100})\right]} \quad (23)$$

By damping coefficient and using the following equations the natural frequency can be obtained:

$$\omega = \frac{\pi}{T_P\sqrt{1-\zeta^2}} \quad (24)$$

$$\omega = \frac{4}{\zeta T_S} \quad (25)$$

3.5. Obtain the poles:

By considering the transfer function of second order answer and using the following the equation we can determine the location of poles in the coordinate plane.

$$S_{1,2} = \xi\omega \pm \omega\sqrt{1-\xi^2} \quad (26)$$

3.6. Pitch Controller

According to the vessel specifications:
Fin Lift= Mfs = -1575.9 kg.m2/s
Iy=469 kg/m2
Added Mass =Mq.= -458 kg.m2
Combined Term = Mq = 9826.2 kg.m2/s
Hydrostatic= Mθ = 13719.6 kg.m2/s2
And using $G_\theta(s)$, the Open loop transfer function is as follows:

$$G_\theta(s) = \frac{-1.7}{s^2+10.6s+14.8} \quad (27)$$

And the open loop poles are:

S1= -1.654 S2 =-8.945

Given that the vessels depth changes should not be too much the overshoot chosen around 0.05. By using $G_\theta(s)$, the value of $\zeta = 0.69$ and the value of T_d= 0.21 was obtained. By using the transfer function Root-Locus graph that we draw in MATLAB, the natural frequency ω_n=1.27 rad/sec and K_p=0.2604 obtained.

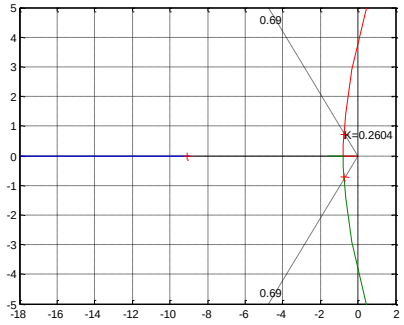

Fig.3 Transfer Function's Root-Locus Graph

3.7. Depth Controller

The depth transfer function adds third pole to the system. To ensure that the Pitch loop response is faster than depth loop response, the Pitch loop poles must be five-time interval away from the depth loop pole. For this we use a graph of the root-Lucas has achieved the appropriate Δ.

3.7.1. State feedback controller

In this section we use state feedback controller with trigger signal, u = -Kx. Where K is gain matrix and x is state matrix.
We have:

$$G_\theta(s) = \frac{-1.7}{s^2+10.6s+14.8} \quad (28)$$

And

$$G_z = {}^{-20}/_{s} \quad (29)$$

That gives us:

$$G_\theta(s) \times G_z = \frac{34}{s^3+10.6s^2+14.8s} \quad (30)$$

[A, B, C, D] = tf2ss ([34],[1 10.6 14.8 0]) (31)
gives:

$$A=\begin{bmatrix}-10.6 & -14.8 & 0\\ 1 & 0 & 0\\ 0 & 1 & 0\end{bmatrix} \quad B=\begin{bmatrix}1\\0\\0\end{bmatrix} \quad C=[0 \quad 0 \quad 34]$$

D= 0 (32)

[DOR: 20.1001.1.25382667.2016.4.0.3.7]

The controllability matrix $P_C = [B \quad AB \quad A^2B]$ is calculated. If the P_c be a non-zero matrix, which means the system is state controllable.

For $\zeta = 0.69$ the poles are $\begin{cases} -0.338 \pm \mathrm{j}\, 0.355 \\ -10 \end{cases}$ and gives us $s^3 + 10.676s^2 + 7s + 2.4 = 0$.

When the matrix A is not in CCF form, we use $\bar{x} =$ Px to transfer the system to CCF form. Then the matrix P is $[0, 0, 1;\ 0, 1, 0;\ 1, 0, 0]$ and the effective system is $(-10.6, -14.8, 0)$. So the gain matrix is as following:

$$K = [10.676 + 1.09, , 7 + 0.52, 2.4 - 0\ ]$$

and

$$P = [11.766, 7.52, 2.4]$$

4. Simulation results

In order to demonstrate the effectiveness and stability of P-PD controller designed in this paper, we tested the maneuverability of selected AUV that we described the specification in section 3.6. One of the most important maneuvers that the underwater vessels do is circulation maneuver that is done by rudders level control. The maneuver is performed by applying a constant angle to the rudder, the submarine began to rotate and its height start decreases. Another important maneuver for submarines is dive and climb maneuvers. These maneuvers are done by using the elevator control levels. These maneuvers change the AUV's depth.

Two of the most important control levels in submarines are rudder control levels (dr) and elevator control levels (ds). The elevator control levels are control the depth means by applying positive and negative input the vessel will climb and dive. As shown in figures 4, 5 and 6 by using positive ds as controller input after 100 seconds the submarine depth changes from 0 to 43 meters. By applying negative ds in designed controller, the submarine start diving gently (figures 7, 8 and 9). By changing the rudder control elevators we can control the submarines heading. In the figures 10 and 11 by applying dr= 0.1 the submarines do the snake maneuver without any change in depth. The figure 12 shows the Snake maneuver in 3-D plot. By applying both rudder control levels and elevator control levels the submarines do the Circulate maneuver that shows in figures 13 and 14.

4.1. Simulation results for d_s= 0.1 (rad)

As mentioned before, for positive elevator control levels input the submarine began climb. The simulation results show below:

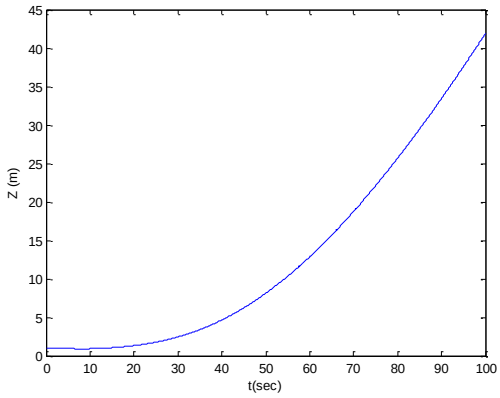

Fig.4 The depth change with time

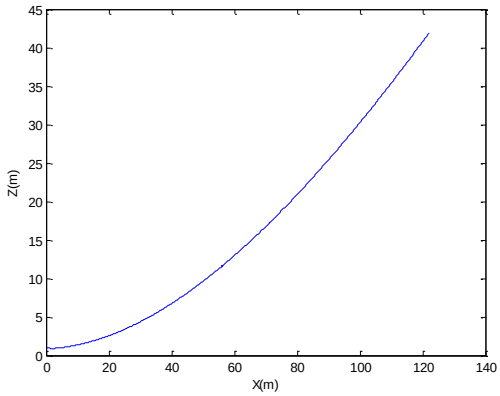

Fig. 5 Moving track in x-z plane

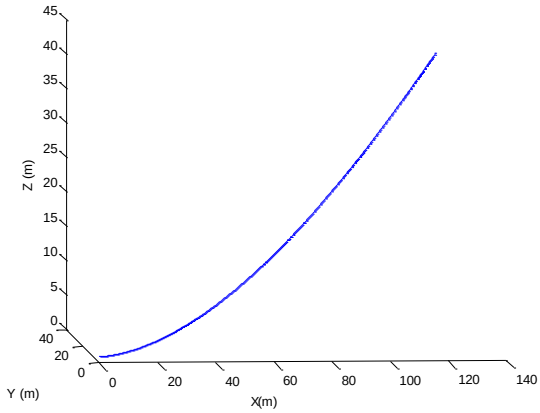

Fig.6 Depth changes in 3-D graph

4.2. Simulation results for d_s= -0.1 (rad)

For negative elevator control levels input the submarine began dive. The simulation results show below. As is evident from the results for asymmetric control orders, the AUV shown symmetric behavior, which represents the accuracy of the simulation.

[DOR: 20.1001.1.25382667.2016.4.0.3.7]

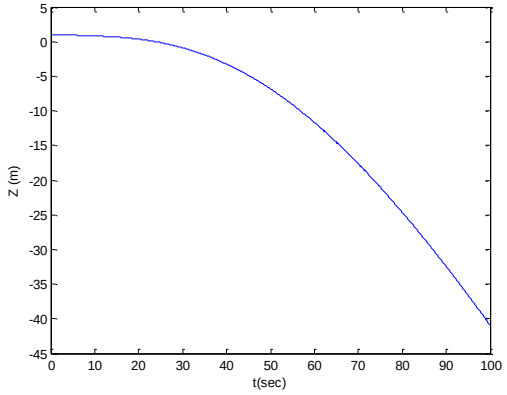

Fig.7 The depth change with ti

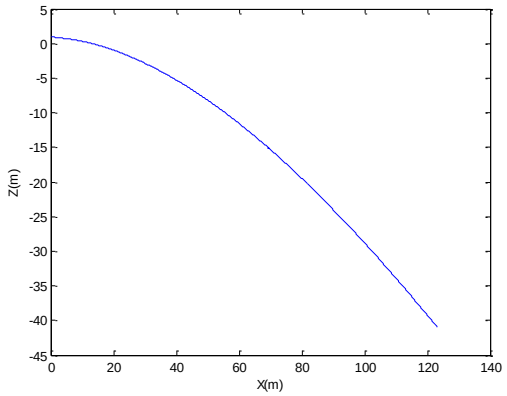

Fig.8 Moving track in x-z plane

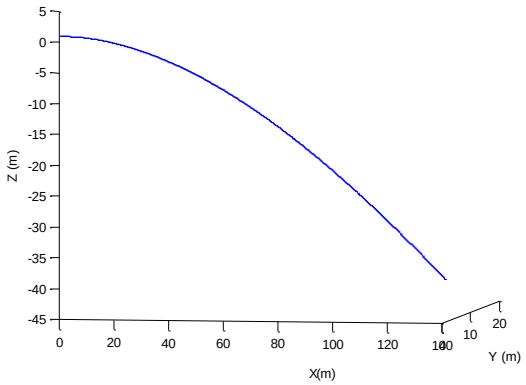

Fig.9 Depth changes in 3-D graph

4.3. Simulation results for dr= 0.1 (rad)

For the rudder control input, submarines began to rotate that the results are shown below:

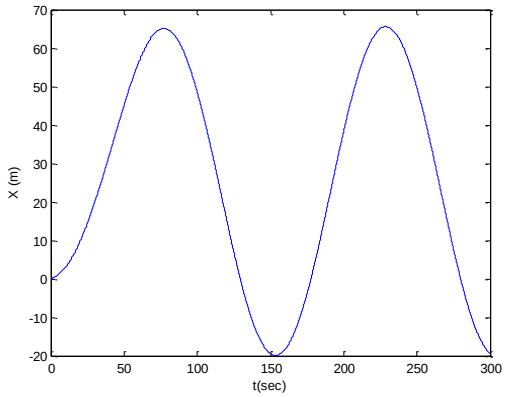

Fig.10 Snake move along the X axis

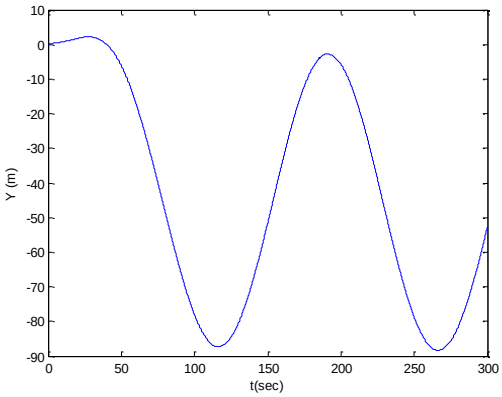

Fig.11Snake move along the Y axis

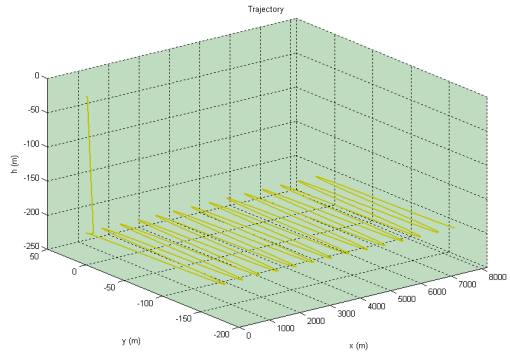

Fig.12The Snake maneuver in 3-D

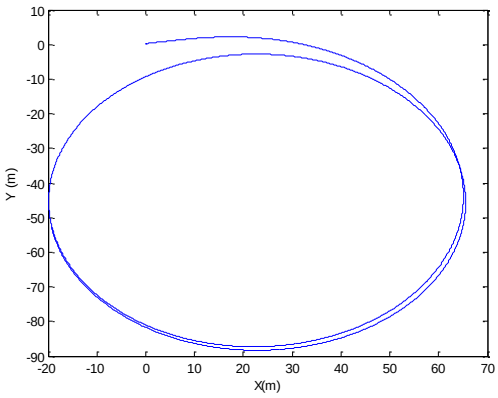

Fig.13 Circulation maneuver in Y-X plane

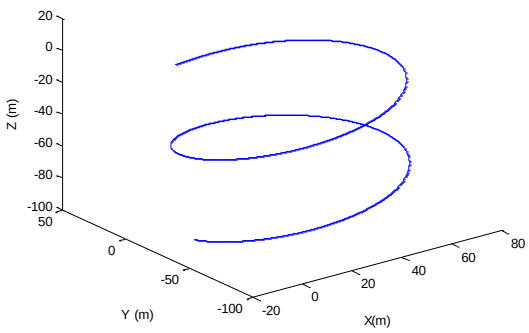

Fig.14 Circulation maneuver in 3-D

[DOR: 20.1001.1.25382667.2016.4.0.3.7]

5. Conclusions

Control systems for depth and heading control of a small AUV were designed and tested in field. The P-PD with state feedback has proved useful in the development of the control systems for the AUV based on Myring hull profile. To construct the control system, a 6 DOF general mathematical model of underwater vehicles was derived, which is powerful enough to apply it to different kinds of underwater vehicles according to its own physical properties. Based on the general mathematical model, a simulation platform was established to test motion characteristics, stability and controllability of the vehicle. The control system was design based on AUV's mathematical model. After that we test the control system performance by dive, climb and circulation orders. The results show that the performance of controllers meets the requirement of performance and stability in both the vertical and horizontal planes.

6. References

[1] Farrell JA, Pang S, Li W, Arrieta R (2004) Biologically inspired chemical plume tracing demonstrated on an autonomous underwater vehicle, Man, and Cybernetics Conference, September 2004, Hague, Netherlands

[2] Yildiz O, Gokalp RB, Yilmaz AE (2009) A review on motion control of the Underwater Vehicles. In: Proceedings of electrical and electronics engineering, 2009. ELECO 2009, Bursa, 2009, pp 337–341

[3] UUV programs (2007) http://ftp.fas.org/irp/program/collect/ uuv.htm

[4] Prestero T Verification of a six-degree-of-freedom simulation model for the REMUS autonomous underwater vehicle, MSc/ME Thesis, Massachusetts Institute of Technology, 2001

[5] Geisbert JS Hydrodynamic modeling for autonomous underwater vehicles using computational and semi-empirical methods. Verginia Polytechnis Institute and State University, 2007

[6] Yue C, Guo S, Li M ,ANSYS fluent-based modeling and hydrodynamic analysis for a spherical Underwater robot. In: Proceedings of 2012 IEEE international conference on mechatronics and automation, pp 1577–1581, 2012

[7] Guo S, Mao S, Shi L, Li M ,Design and kinematic analysis of an amphibious spherical robot. In: Proceedings of 2012 IEEE international conference on mechatronics and automation, pp 2214–2219, 2012

[8] Herman P ,Decoupled PD set-point controller for underwater vehicles. J Ocean Eng 36(6–7):529–534,2009

[9] Fossen, T.I . Guidance and Control of Ocean Vehicle . New York: John Wiley & Sons. 1994

[10] Wadoo S, Kachroo , Autonomous underwater vehicles: modeling, control design and simulation. CRC Press, edn 1,2010

[11] Buckham BJ, Podhorodeski RP, Soylu S , A chattering-free sliding-mode controller for underwater vehicles with fault tolerant infinity-norm thrust allocation. J Ocean Eng, 35(16):1647–1659, 2008

[12] Qi X, Adaptive coordinated tracking control of multiple autonomous underwater vehicles. Ocean Eng 91:84–90, 2014

[13] Zeinali M, Notash L, Adaptive sliding mode control with uncertainty estimator for robot manipulators. Mech Mach Theory 45(1):80–90, 2010

[14] Jun SW, Kim DW, Lee HJ, Design of T-S fuzzy-model based controller for depth control of autonomous underwater vehicles with parametric uncertainties. In: 2011 11th international conference on control, automation and systems, ICCAS 2011, Gyeonggi-do, Korea, Republic of, 2011, pp 1682–1684,2011

[15] Kumar N, Panwar V, Sukavanam N, Sharma SP, Borm JH, Neural network-based nonlinear tracking control of kinematically redundant robot manipulators. Math Compute Model 53(9–10):1889–1901, 2011

[16] Fossen, T.I . Marine Control System . 2002

[17] Xu B, Pandian SR, Sakagami N, Petry F, Neuro-fuzzy control of underwater vehicle-manipulator systems. J Franklin Institute, 349(3):1125–1138,2012

[18] Medagoda L, Williams SB, Model predictive control of an autonomous underwater vehicle in an in situ estimated water current profile. Oceans, Yeosu, pp 1–8, 2012

[19] Steenson LV, Phillips AB, Turnock SR, Furlong ME, Rogers E, Effect of measurement noise on the performance of a depth and pitch controller using the model predictive control method. Autonomous underwater vehicles (AUV), 2012 IEEE/ OES, 1(8):24-27, 2012

[20] Mohan S, Kim J, Indirect adaptive control of an autonomous underwater vehicle-manipulator system for underwater manipulation tasks. Original Res Article Ocean Eng 54(1):233–243, 2012

[21] Cooney LA, Dynamic response and maneuvering strategies of a hybrid autonomous underwater vehicle in hovering. Thesis of Master of Science in ocean engineering, Massachusetts Institute of Technology, 2009

[22] Sgarioto D, Steady state trim and open loop stability analysis for the REMUS autonomous underwater vehicle. Defense Technology Agency, New Zealand Defense Force, DTA Report 254, 2008

[23] Yang C, Modular modeling and control for autonomous underwater vehicle (AUV). Thesis of master of engineering department of mechanical engineering national university of Singapore, 2007

[24] Lin FC, Adaptive fuzzy logic-based velocity observer for servo motor drives. Mechatronics 13:229–241, 2003

[25] Subudhi B, Mukherjee K, Ghosh S, A static output feedback control design for path following of

[DOR: 20.1001.1.25382667.2016.4.0.3.7]

autonomous underwater vehicle in vertical plane. Ocean Eng 63:72–76, 2013

[26] A. Annamalai, A. Motwani, S.K. Sharma, R. Sutton,P. Culverhouse and C. Yang, A Robust Navigation Technique for Integration in the Guidance and Control of an Uninhabited Surface Vehicle, THE JOURNAL OF NAVIGATION, 68, 750–768, 2015

[27] Bong SeokPark, Adaptive formation control of under actuated autonomous underwater vehicles, Elsevier, Ocean Engineering96, 2015

[28] Thor I. Fossen, and Anastasios M. Lekkas, Direct and indirect adaptive integral line-of-sight path-following controllers for marine craft exposed to ocean currents, INTERNATIONAL JOURNAL OF ADAPTIVE CONTROL AND SIGNAL PROCESSING, 2015

[29] M. Kim, Hangil Joe and Son-Ceol Yu, Dual-loop robust controller design for autonomous underwater vehicle under unknown environmental disturbances, ELECTRONICS LETTERS, Vol. 52, No. 5, pp. 350–352, 2016

[DOR: 20.1001.1.25382667.2016.4.0.3.7]